THIN FILMS MADE FROM COLLOIDAL ANTIMONY TIN OXIDE NANOPARTICLES FOR TRANSPARENT CONDUCTIVE APPLICATIONS

A Thesis Presented to
The Academic Faculty

by

Abigail Halim

In Partial Fulfillment
of the Requirements for the Degree
Bachelor of Science in the
School of Materials Science and Engineering

Georgia Institute of Technology
May 2013

THIN FILMS MADE FROM COLLOIDAL ANTIMONY TIN OXIDE NANOPARTICLES FOR TRANSPARENT CONDUCTIVE APPLICATIONS

Approved by:

Dr. Rosario Gerhardt, Advisor
School of Materials Science and Engineering
Georgia Institute of Technology

Dr. Dong Qin
School of Materials Science and Engineering
Georgia Institute of Technology

Dr. Fred Cook
School of Materials Science and Engineering
Georgia Institute of Technology

Date Approved: April 26, 2013

ACKNOWLEDGMENTS

I would like to thank Dr. Gerhardt for her guidance and support and Danny Jeong, Salil Joshi, Tim Pruyn, Rachel Muhlbauer, Chunqing Peng, and Justin Brandt for training me on various instruments and answering my questions. I would also like to thank Dr. Kroger for allowing me to use his Zetasizer and Nick Haase for training and helping me in using the Zetasizer. Lastly, I would like to thank Exide Technologies for funding this project through a research scholarship and the Institute President's Office for granting a salary and travel award through the President's Undergraduate Research Award.

TABLE OF CONTENTS

LIST OF TABLES

LIST OF FIGURES

LIST OF SYMBOLS AND ABBREVIATIONS

ATO	antimony tin oxide
TMAH	tetramethylammonium hydroxide
ITO	indium tin oxide
TCO	transparent conducting oxide

SUMMARY

In this study, antimony tin oxide (ATO) nanoparticles from Alfa Aesar were redispersed in water using tetramethylammonium hydroxide (TMAH) as a dispersing agent and deposited onto glass substrates by spin coating. Films of one to five layers were made. These thin films were characterized using impedance spectroscopy and ultraviolet-visible spectroscopy to obtain their resistances and optical transmittance, respectively. The films displayed sheet resistances around 10^5-10^4 kΩ/□ and optical transmittance in the near infrared to near ultraviolet range above 95%. Films were then made using a higher concentration ATO solution and found to achieve sheet resistances on the order of 10^2 kΩ/□. Impedance measurements, along with optical micrographs, were taken at different locations on the films, demonstrating that films of more than one layer showed greater uniformity. Further sets of films were also produced with varying substrate preparation and dispersion deposition parameters. Aside from dispersion concentration, high humidity during film measurement was found to be the most crucial parameter for achieving low sheet resistances.

CHAPTER 1

INTRODUCTION

Oxide thin films have gained much attention for transparent conductive applications due to their unique electrical and optical properties. Indium tin oxide (ITO) thin films have become an industry standard but require scarce, expensive materials to produce. Antimony-doped tin oxide thin films are also being studied as an alternative, as they have properties comparable to ITO thin films and are less expensive.

CHAPTER 2

LITERATURE REVIEW

Transparent Conducting Oxides

Transparent conducting oxides (TCOs) are thin films of metal oxides that exhibit both optical transparency and electrical conductivity [1]. For these reasons, they have become widely used in applications such as solar cells, light emitting diodes, and liquid crystal displays [2]. The first TCO was discovered over a century ago when a sputter deposited cadmium thin film underwent incomplete thermal oxidation with post-deposition heating in air [3]. Since this realization, many other TCO materials have been developed, namely n-type semiconductors with tin oxide, indium oxide, or zinc oxide as the main component, displayed in Table 2.1 [1].

Table 2.1 Common TCO Materials

Main Component	Dopant
Tin Oxide (SnO_2)	Fluorine (F)
	Antimony (Sb)
Indium Oxide (In_2O_3)	Tin (Sn)
	Zinc (Zn)
Zinc Oxide (ZnO)	Aluminum (Al)
	Boron (B)
	Gallium (Ga)

The key to attaining both optical transparency and electrical conductivity in TCOs is the nature of the energy band gap in degenerate semiconductors. To overcome the band gap, electrical conductivity in TCOs is achieved by increasing the number of free charge carriers through intrinsic defects, such as oxygen vacancies, or through extrinsic dopants, typically higher-valency metal cations [2]. In n-type semiconductors, these dopants or defects provide energy levels close to the bottom of the conduction band, allowing those electrons to get promoted into the conduction band as free charge carriers. In p-type semiconductors, the additional energy levels lie close to the valence band, allowing electrons to be promoted into the extra energy levels and creating holes in the valence band to act as free charge carriers [3].

The optical transparency of TCOs is made possible by the existence and magnitude of the energy band gap. Unlike metals, there exists a range of wavelengths for which electrons cannot absorb light due to their corresponding energies and the semiconductor band gap energy [4]. This creates a transmission boundary in the near-ultraviolet region, above which light has enough energy to promote an electron in the valence band into the conduction band [2]. The lower energy boundary appears in the near-infrared region, below which transmission is restricted due to absorption of light by electronic transitions between energy levels within the valence band [3].

Indium tin oxide (ITO) is an In_2O_3-rich compound of In_2O_3 and SnO_2 that has become the principal TCO material as a result of its excellent optical and electrical properties, having average resistivities of about $1 \times 10^{-4}\ \Omega \cdot cm$ [2]. However, alternatives to ITO are being investigated because of the high cost and scarcity of indium. Fluorine-doped tin oxide (FTO) is the second most used TCO, but it has a

relatively low electrical conductivity and is more difficult to pattern using wet-etching [2]. Aluminum- and gallium-doped zinc oxides (AZO and GZO, respectively) are also good alternatives to ITO, but they tend to degrade faster than ITO and FTO in hot, moist atmospheres [2].

Antimony Tin Oxide TCOs

Antimony tin oxide (ATO) is a TCO material whose properties have been studied and looks to be a promising alternative to ITO due to its low cost [5-12]. Where ITO is Sn-doped indium oxide, ATO is Sb-doped tin oxide (SnO_2). SnO_2 has a rutile crystal structure, with Sn atoms in the corner and center positions and oxygen atoms occupying the tetrahedral interstitial sites [13]. In ATO, Sb cations substitute for the Sn^{4+} cations. With low amounts of Sb doping, Sb^{5+} ions dominate, decreasing resistivity by increasing the free carrier density with excess electrons. With increased doping (above 5 wt.% Sb), Sb^{5+} is reduced to Sb^{3+}, and Sb^{3+} ions begin to dominate, increasing resistivity [14].

Table 2.2 displays a summary of the optimal electrical and optical properties obtained from ATO thin films of different compositions using a variety of deposition techniques.

Table 2.2 Summary of ATO Thin Film Properties

Deposition Technique	Composition	Resistivity/Sheet Resistance	Transmission	Reference
Sol-gel spinning	30 at.% Sb	1.19×10^{-3} Ω·cm	92.5% at 0.55 μm	5
Spin coating	5 mol% Sb	1.7×10^{-2} Ω·cm	>90% in visible range	6
Spray pyrolysis	0.5 mol% Sb	2.57×10^{-3} Ω·cm	~90% in visible and near-IR range	7
Solvothermal	15 at.% Sb	9.0×10^{5} Ω/□	-	8
Reactive DC magnetron sputtering	5 wt.% Sb	3.3×10^{-3} Ω·cm	74% in visible range	9
Perfume atomizer	2 at.% Sb 40 at.% F	3.27×10^{-4} Ω·cm	76% in visible range	10
Oblique angle deposition	7 wt.% Sb	9.0×10^{2} Ω/□	~90% in visible range	11
Sol-gel dip-coating	15 mol% Sb	1.0×10^{2} Ω/□	-	12

While the resistivities and transmission for ATO thin films that have been recorded are close to those of their ITO counterparts, they still fall behind the lower resistivities and higher transmission of ITO. To be able to compete with ITO, ATO thin films also need to be more easily manufactured. This study proposes to promote the use of ATO by optimizing the fabrication of ATO thin films by solution-processing commercially-available ATO nanoparticles.

CHAPTER 3

MATERIALS AND METHODS

Dispersion Preparation

ATO (Alfa-Aesar) nanoparticles were redispersed in water using tetramethylammonium hydroxide (TMAH) as a dispersing agent. The ATO powder was massed and combined with 10 wt.% TMAH solution (Sigma-Aldrich) in a ratio of 0.1823 µL of TMAH solution per mg of ATO [6]. Water was added to adjust the ATO dispersion concentration, and the dispersion was sonicated for 10 minutes and stirred until deposition. Dispersions of 0.1 wt.% and 5 wt.% were made.

Film Deposition

Microscope slides were cut into 1” x 1” substrates and cleaned using Kimwipes and pure water, acetone, and isopropyl alcohol. The substrates were treated with UV ozone at 50°C for 15 minutes. Spin coating was used to deposit the ATO dispersion onto the substrates. The spin coating program used was an initial speed of 2000 rpm accelerated at 100 r/s for 45 s., followed by a drying speed of 5000 rpm accelerated at 1000 r/s for 30 s. To form one layer of ATO film using spin coating, 200 µL of the ATO suspension was pipetted onto the center of the substrate before starting the spin coating program. To ensure all water had been removed before deposition of further layers, the films were placed in a furnace set to 90-100°C for 10 minutes between each layer deposition. Films of one to five layers were made.

Varying Substrate Preparation and Film Deposition Parameters

The importance of UV-ozone treatment for substrate preparation was studied by exposing some substrates to UV ozone at 50°C for 15 minutes and leaving other substrates untreated. The deposition conditions studied were pipetting the dispersion onto the substrate before starting the spin coating program, while the substrate was motionless, and pipetting the dispersion 3 s. into the spin coating program, while the substrate had a velocity of about 300 rpm.

Film Characterization

The thin films were characterized using impedance spectroscopy to obtain their sheet resistances. A Solartron 1296 and Solartron 1260 were used to take four point probe measurements on the samples. Measurements were taken between probes 1-2, 2-3, and 3-4 in at least one of the positions shown in Figure 3.1. The sheet resistances were calculated by fitting the first semicircle in the complex impedance graph from the impedance data to a simple equivalent circuit of a resistor in parallel with a constant phase element. All measurements from one film were averaged to obtain the representative sheet resistance of each film. Optical microscopy was used to investigate the film structures and uniformity.

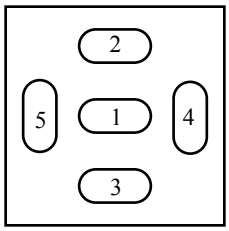

Figure 3.1. Schematic of the five positions used on the films to place the four point probe for impedance measurements.

CHAPTER 4

RESULTS AND DISCUSSION

Sheet resistances of films made with 0.1 wt.% and 5 wt.% ATO dispersions are displayed in Figure 4.1a. Examples of the impedance curves for the 5 wt.% films from which the sheet resistances were calculated are shown in Figure 4.1b.

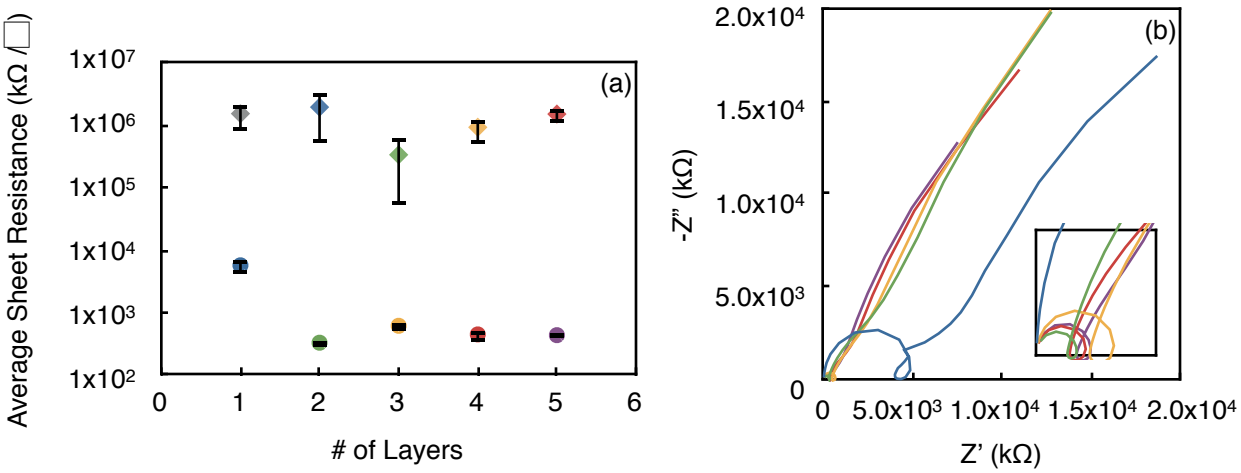

Figure 4.1 a) Average sheet resistances of ATO thin films of one to five layers, with diamonds showing 0.1 wt.% films and circles showing 5 wt.% films and b) representative impedance graphs of films made with 5 wt.% ATO dispersion. Inset shows a larger view of the semicircles for films of 2-5 layers.

All 0.1 wt.% films showed high sheet resistances on the order of 10^6 kΩ/□, indicating that the ATO nanoparticles did not form a continuous network in the film. It can clearly be seen that increasing the dispersion concentration drastically affects the sheet resistance, decreasing it by about four orders of magnitude. With the 5 wt.% films, the

sheet resistances level out after two layers. This may be due to repulsion of the film and the dispersion, preventing the actual addition of further layers.

Optical micrographs of the 5 wt.% films are displayed in Figure 4.2.

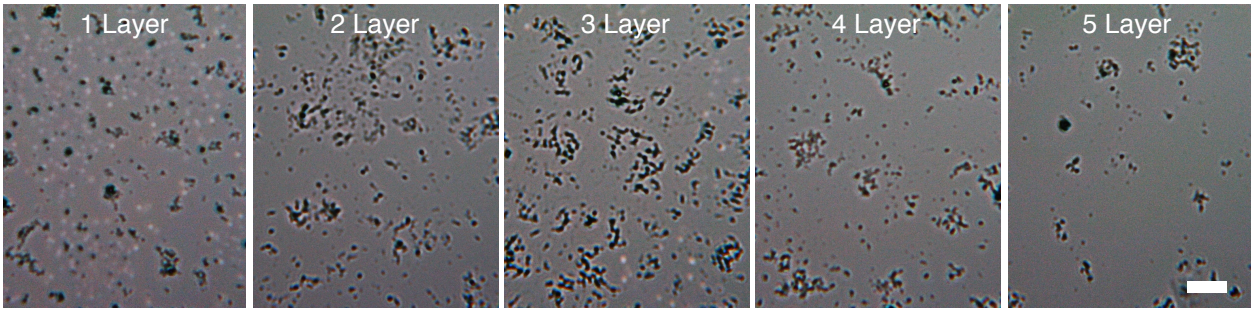

Figure 4.2 Optical micrographs of films made with 5 wt.% ATO dispersion. 10μm scale bar applies to all images.

The micrographs show that all films are fairly uniform and exhibit the same structure. The visible formations are likely aggregates of the ATO nanoparticles. Single nanoparticles are not visible on this scale and could be spread throughout the regions between the aggregates.

Figure 4.3 presents the transmittance of the 0.1 wt.% and 5 wt.% films.

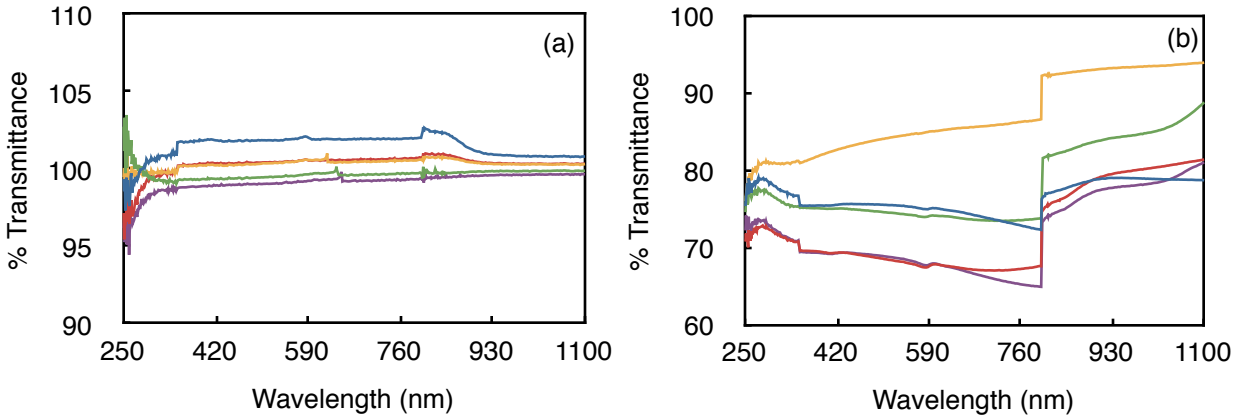

Figure 4.3 Transmittance spectra of ATO films of 1-5 layers made with a) 0.1 wt.% and b) 5 wt.% ATO dispersions.

A substantial decrease in transmittance can be seen when the dispersion concentration is increased from 0.1 wt.% to 5 wt.%. This decrease is understandable, as more nanoparticles are deposited onto the substrate when using a higher concentration.

Effects of Substrate Preparation and Deposition Parameters

When studying the effects of UV-ozone treatment and of deposition before or after the start of the spin coating program, minor differences in properties were detected. The sheet resistances and photographs of films with different preparation parameters are shown in Figure 4.4.

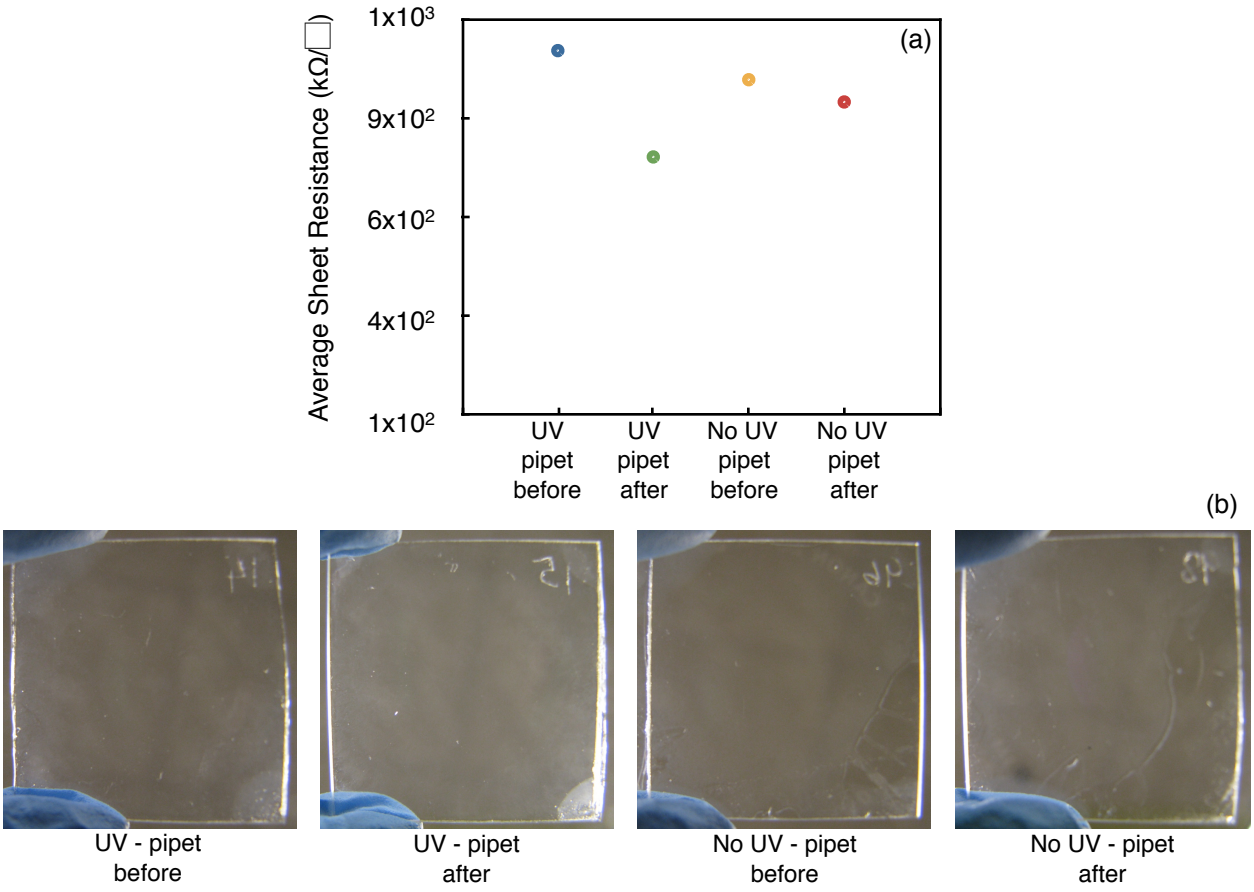

Figure 4.4 a) Average sheet resistances and b) photographs of films with varying substrate preparation and dispersion deposition parameters.

The lowest sheet resistance was obtained with a substrate prepared with UV-ozone and deposition after starting the spin coating program. Treating the glass with UV-ozone activates the surface, making it more hydrophilic and enabling the aqueous dispersion of ATO nanoparticles to better adhere to the glass. The films on UV-ozone treated substrates also looked more uniform and completely covered the substrate surface, whereas the other films left some of the glass surface uncovered.

Effect of Humidity

When attempting to reproduce the films with sheet resistances on the order of 10^2 kΩ/□, some experiments resulted in films of higher sheet resistances by five orders of magnitude. All substrate preparation, dispersion preparation, and deposition parameters were kept constant, so other factors were investigated. It was found that relative humidity during measurement significantly affected the sheet resistances of the films. The sheet resistances and representative impedance graphs of the same films measured at low and high relative humidities are displayed in Figure 4.5.

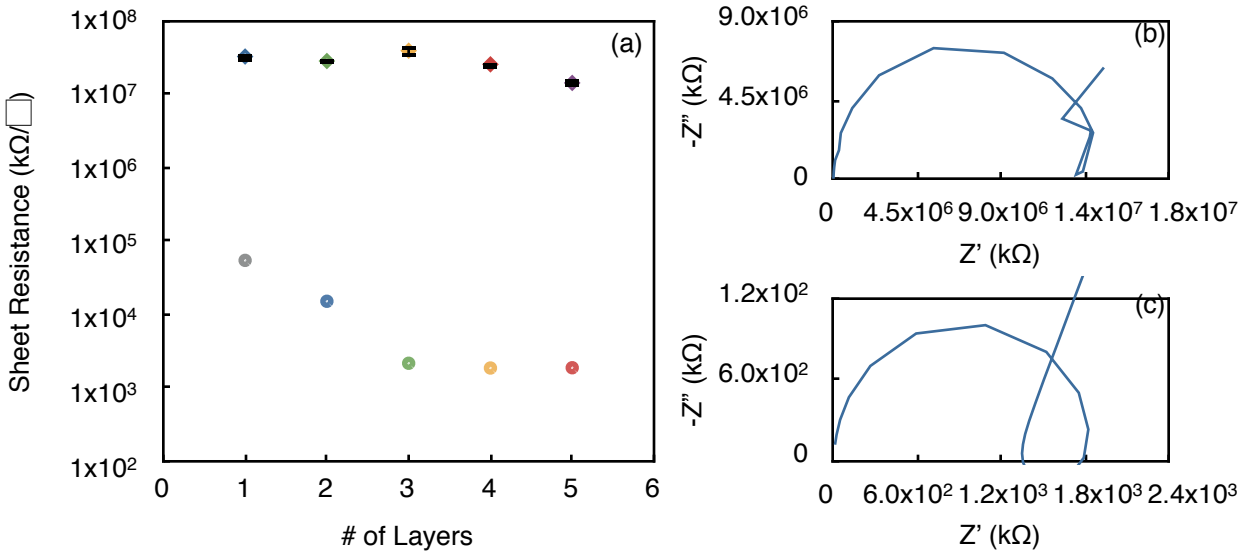

Figure 4.5 a) Sheet resistances of films measured at low (diamonds) and high (circles) relative humidities. Impedance plots of 5 layer films measured with b) low and c) high relative humidities.

It is evident that films measured at a higher relative humidity had lower sheet resistances. It is unclear why this change in properties occurs, but it is likely related to the residual TMAH that is contained in the films.

CHAPTER 5

CONCLUSIONS

Films of sheet resistances on the order of 10^2 kΩ/□ were produced using solution processed commercial ATO nanoparticles. Increasing the ATO dispersion concentration decreased the sheet resistances of the films. Although deliberately varying substrate preparation and deposition parameters had some effect on film properties, the most important factor in producing low or high sheet resistance films was relative humidity during film measurement.

Although the ATO films produced in this study did not show comparable properties to those of ITO films, the decrease in sheet resistances achieved by varying processing parameters shows promise in further reducing the ATO sheet resistances to values necessary for current applications. For application environments like solar cells, it would also be necessary to eliminate the effect of relative humidity on the ATO film properties, as relative humidity would constantly vary in open air. This would likely require the removal of residual TMAH from the film while maintaining film structure and uniformity. With further studies to resolve these issues, commercial ATO nanoparticles could potentially be solution-processed into transparent conductive films.

REFERENCES

[1] S. Calnan and A. N. Tiwari (2010). "Review: High mobility transparent conducting oxides for thin film solar cells." Thin Solid Films **518**: 1839-1849.

[2] H. Liu, V. Avrutin, N. Izyumskaya, U. Ozgur, and H. Morkoc (2010). "Review: Transparent conducting oxides for electrode applications in light emitting and absorbing devices." Superlattices and Microstructures **48**: 458-484.

[3] G. J. Exarhos and X. Zhou (2007). "Review: Discovery-based design of transparent conducting oxide films." Thin Solid Films **515**: 7025-7052.

[4] Schaffer, Saxena, Antolovich, Sanders, Warner (2010). The Science and Design of Engineering Materials, McGraw-Hill.

[5] L. K. Dua, A. De, S. Chakraborty, and P. K. Biswas (2008). "Study of spin coated high antimony content Sn-Sb oxide films on silica glass." Materials Characterization **59**(5): 578-586.

[6] C. Goebbert, R. Nonninger, M. A. Aegerter, and H. Schmidt (1999). "Wet chemical deposition of ATO and ITO coatings using crystalline nanoparticles redispersable in solutions." Thin Solid Films **351**(1-2): 79-84.

[7] G. Jain and R. Kumar (2004). "Electrical and optical properties of tin oxide and antimony doped tin oxide films." Optical Materials **26**(1): 27-31.

[8] H. J. Jeon, M. K. Jeon, M. Kang, S. G. Lee, Y. L. Lee, Y. K. Hong, and B. H. Choi (2005). "Synthesis and characterization of antimony-doped tin oxide (ATO) with nanometer-sized particles and their conductivities." Materials Letters **59**(14-15): 1801-1810.

[9] J. Montero, C. Guillen, and J. Herrero (2011). "Discharge power dependence of structural, optical and electrical properties of DC sputtered antimony doped tin oxide (ATO) films." Solar Energy Materials and Solar Cells **95**(8): 2113-2119.

[10] K. Ravichandran and P. Philominathan (2008). "Fabrication of antimony doped tin oxide (ATO) films by an inexpensive, simplified spray technique using perfume atomizer." Materials Letters **62**(17-18): 2980-2983.

[11] X. Xiao, G. Dong, J. Shao, H. He, and Z. Fan (2010). "Optical and electrical properties of SnO_2:Sb thin films deposited by oblique angle deposition." Applied Surface Science **256**(6): 1636-1640.

[12] D. Zhang, Z. Deng, J. Zhang, and L. Chen (2006). "Microstructure and electrical properties of antimony-doped tin oxide thin film deposited by sol-gel process." Materials Chemistry and Physics **98**(2-3): 353-357.

[13] G. Qin, D. Li, Z. Chen, Y. Hou, Z. Feng, and S. Liu (2009). "Structural, electronic and optical properties of $Sn_{1-x}Sb_xO_2$." Computational Materials Science **46**(2): 418-424.

[14] T. Krishnakumar, R. Jayaprakash, N. Pinna, A. R. Phani, M. Passacantando, and S. Santucci (2009). "Structural, optical and electrical characterization of antimony-substituted tin oxide nanoparticles." Journal of Physics and Chemistry of Solids **70**: 993-999.